Properties of lateral Nb contacts to a two-dimensional electron gas in an $In_{0.77}Ga_{0.23}As/InP$ heterostructure

K. Neurohr, A. A. Golubov,* Th. Klocke, J. Kaufmann, Th. Schäpers, J. Appenzeller, D. Uhlisch, A. V. Ustinov, M. Hollfelder, H. Lüth, and A. I. Braginski
Institute of Thin Film and Ion Technology, Research Centre Jülich (KFA), D-52425 Jülich, Germany
(Received 11 June 1996; revised manuscript 20 August 1996)

We have measured the differential resistance of lateral Nb contacts to a two-dimensional electron gas (2DEG) in an $InP/In_xGa_{1-x}As$ heterostructure. The I-V curves show strong deviations from the frequently used model developed by Blonder, Tinkham, and Klapwijk. In all samples the maximum of conductance at about $eV=\Delta_0$ is damped and shifted to lower voltages. Depending on the surface cleaning procedure two different regimes are observed. We will present two models that allow one to interpret the conductance mechanisms. The parameters used in the models are within a realistic range given by characteristic material values. In the case of wet chemically cleaned samples the 2DEG is assumed to be in the clean limit. To describe the measurement results of these samples we assume a proximity effect in a Nb oxide layer (N) located between the Nb (S) and the 2DEG causing the shift of the conductance maximum. Pair-breaking processes in this SN electrode are responsible for the damping of this maximum. Additionally we include the proximity effect between the electrode and the 2DEG in our model. When the semiconductor surface is cleaned by Ar ions, the 2DEG is damaged at the surface. For this case we have shown that an additional voltage drop occurs in this disturbed part of the 2DEG and that the inelastic scattering in the SN electrode is stronger than in the case of the wet chemically cleaned samples. [S0163-1829(96)06544-7]

I. INTRODUCTION

After the proposal of a Josephson field effect transistor (JOFET) based on the superconducting proximity effect in a semiconductor between two superconducting banks,[1] initial attempts of experimental realization dealt with highly doped semiconductors combined with low-T_C superconductors like Nb or Pb. The high carrier concentration in the semiconductor results in a strong proximity effect which was, for example, observed in p-Si,[2] n-InAs (Ref. 3), and in the surface accumulation layer of p-InAs.[4] The next step was the use of heterostructures with a two-dimensional electron gas (2DEG). They combine high mobilities with low effective masses. Especially, the large mean-free-path lengths provide phase coherent transport and, therefore, high critical currents in S-Sm-S devices. Depending on the material, heterostructures have several advantages for hybrid devices, but also yield some problems. The $Al_xGa_{1-x}As/GaAs$ heterostructures show very high mobilities[5,6] but the superconducting electrodes have to be alloyed in order to avoid formation of a Schottky barrier at the surface of the GaAs. Furthermore, Al leads to technological problems due to oxidation. An $In_xAl_{1-x}As/In_xGa_{1-x}As$ heterostructure with an inserted InAs channel is typically characterized by high electron concentrations and an accumulation layer at the channel surface but does not reach the high mobilities of $Al_xGa_{1-x}As/GaAs$ heterostructures. Nevertheless, the big advantage of this system is the accumulation layer which allows for a good contact of the superconductor to the 2DEG at the etched side walls.[7] Best transport properties are obtained with $InAs/Al_xGa_{1-x}Sb$ heterostructures,[8] but again, Al and especially Sb make it difficult to handle the material system technologically.

A good compromise which allows one to achieve a high mobility in the 2DEG channel and highly transparent interfaces is the use of an $InP/In_xGa_{1-x}As$ heterostructure with a highly strained $In_{0.77}Ga_{0.23}As$ channel. The samples examined in this paper have mobilities of about 370.000 $cm^2/V\,s$, carrier concentrations of about 7×10^{11} cm^{-2}, and an effective mass of $0.037m_e$. Transport measurements on quantum wires in this system showed very low Schottky barriers at the edges of the 2D channel.[9] This enables one to contact the 2DEG with a superconductor without alloying.

To examine the coupling between the niobium electrodes and the 2DEG in a $In_{0.77}Ga_{0.23}As$ channel we measured the differential resistance of a single contact (S-Sm junction). This way of characterizing interfaces between a superconductor and a semiconductor was chosen before, e.g., for Nb-Si,[10,11] Nb-$In_{0.53}Ga_{0.47}As$,[12–14] and Nb-(Al,Ga)Sb (Refs. 15,16) systems. In all these studies the data could not be described by the model developed by Blonder, Tinkham, and Klapwijk (BTK).[17] Also for our samples the measured voltage dependence of the differential resistance showed strong deviations from the predictions of the BTK model. In all samples the maximum of conductance at about $eV=\Delta_0$ is damped and shifted to lower voltages. Depending on the surface cleaning procedure two different regimes are observed. We will present two models that allow to interpret the conductance mechanisms. The parameters used in the models are within a realistic range given by characteristic material values. In the case of wet chemically cleaned samples the 2DEG is assumed to be in the clean limit. To describe the measurement results of these samples we assume a proximity effect in a Nb oxide layer (N) located between the Nb (S) and the 2DEG causing the shift of the conductance maximum. Pair-breaking processes in this SN electrode are re-

0163-1829/96/54(23)/17018(11)/$10.00 © 1996 The American Physical Society

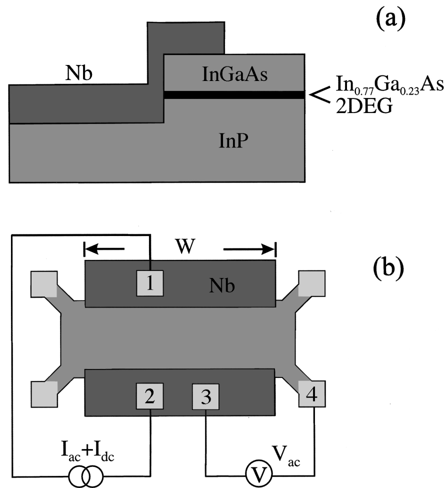

FIG. 1. (a) Schematic cross section of the investigated lateral contact of the Nb film to the 2DEG in a 10-nm-thick $In_{0.77}Ga_{0.23}As$ layer. (b) Schematic top view of the sample layout.

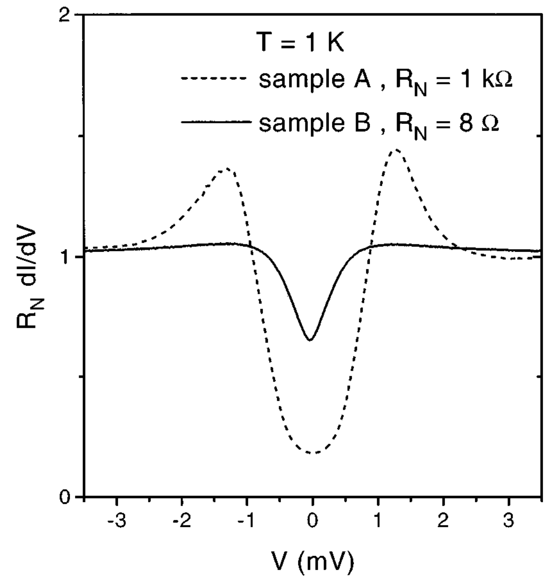

FIG. 2. Normalized differential conductance of the wet chemically cleaned sample A and the sample B cleaned by Ar sputtering plotted versus the voltage drop at the Nb-2DEG interface.

sponsible for the damping of this maximum. Additionally we include the proximity effect between the electrode and the 2DEG in our model. When the semiconductor surface is cleaned by Ar ions, the 2DEG is damaged at the surface. For this case we have shown that an additional voltage drop occurs in this disturbed part of the 2DEG and that the inelastic scattering in the SN electrode is stronger than in the case of the wet chemically cleaned samples. Our main conclusion is that the straightforward use of the BTK model for fitting the experimental data yields an underestimated barrier height between Nb and 2DEG.

II. SAMPLES

For the investigation of the Nb-2DEG contacts we used a modulation-doped $In_{0.77}Ga_{0.23}As$/InP heterostructure with a 2DEG in the ternary compound. The structures were grown by low-pressure metal-organic vapor phase epitaxy (LOMOVPE). They consist of a 10-nm-thick n-doped spike of InP ($N_D=4.9\times10^{17}$ cm^{-3}) on a 300-nm InP buffer, followed by a 20-nm InP spacer layer and a 10-nm thick $In_{0.77}Ga_{0.23As}$ channel, which is finally capped with a 150-nm-thick $In_{0.53}Ga_{0.47}As$ top layer.[18] Due to the high In content, the channel is highly strained. Hall effect measurements of our 2DEG at 1.4 K yield mobilities of about 370 000 cm^2/V s and carrier concentrations of about 7×10^{11} cm^{-2}.

In order to contact the 2DEG laterally with the Nb, the semiconductor was partially removed by reactive ion etching using a CH_4/H_2 process. Subsequently, Ohmic contacts of Ni/AuGe/Ni were alloyed to the 2DEG in order to measure the voltage drop at the interface between 2DEG and Nb [e.g., contact 4 in Fig. 1(b)]. Before Nb deposition, the surface was cleaned either with 1 HF: 20 H_2O (sample type A) or 800-eV Ar ions (sample type B) in order to remove oxides. These oxides remained on the surface after an O_2 plasma treatment that was performed to remove polymers from the semiconductor surface after the reactive ion etching process. In the last step, 100-nm sputtered Nb was deposited and patterned by optical lithography using the standard lift-off technique.

The samples were measured in a ^{3}He-evaporation cryostat. We used the four-terminal configuration and standard lock-in technique to measure the differential resistance of the Nb-2DEG contacts. Figure 1(b) shows a schematic top view of a sample. The current leads 1 and 2 are bonded on two different Nb electrodes, which enable us to drive the current perpendicular to the Nb-2DEG contacts. The distance between the two Nb films is 80 μm, so that any superconducting influence from one Nb electrode to the other one can be neglected. The voltage drop at one Nb-2DEG interface can, e.g., be measured between the voltage probes 3 and 4. The Ohmic contact 4 is well separated from the Nb-2DEG interface which prevents Ni from affecting superconducting properties of the structure. This configuration enables us to measure two independent Nb-2DEG contacts on one sample. The width W of the contacts is 100 μm. Figure 1(a) shows a schematic cross section of one contact. The Nb film has a 3-μm overlap with the $In_xGa_{1-x}As$ cap layer due to the limited accuracy of optical lithography alignment. The leakage current through the 150-nm-thick cap layer can be neglected in our measurements according to a comparative study of top and side contacts to our structures.[19]

III. EXPERIMENTAL RESULTS

Figure 2 shows measured curves for two samples A and B prepared by different cleaning procedures. They are representative for the 30 samples we measured. The differential conductance dI/dV is plotted versus the voltage drop V at the Nb-2DEG interface and is normalized to the resistance value R_N at high bias voltage.

Before depositing Nb, the semiconductor surface of sample A was cleaned by wet chemical etching using HF, which yields $R_N\sim1$ kΩ. The spread in R_N for the 12 samples of this type was quite large, possibly due to inhomogeneities of the barrier along the Nb-2DEG contact. Since it was not possible to heat the samples after the wet chemical

cleaning in our present setup, adsorbates like fluoride and water remained on the surface. This was proven by x-ray photoemission spectroscopy (XPS) on similarly treated test samples. The differential conductance of these contacts can not be interpreted in terms of the classic BTK model ascribing the conductance in the subgap region only to Andreev reflection. In Sec. VI we will show that introducing some extensions of the BTK model helps to fit the experimental curves. The assumption of a normal NbO_x layer between Nb and 2DEG permits one to explain the shift of the conductance maximum at $eV=\Delta_0$ to lower voltages and yields a lower contact transparency than that according to BTK. The reduced height of this conductance maximum can be explained by the presence of inelastic scattering in the Nb electrode.

The 18 samples of type B were cleaned by *in situ* Ar sputtering before deposition of Nb. They show rather homogeneous contacts with a small spread in R_N between 7 Ω and 9 Ω. The lower resistance of sample B is mainly due to a larger effective contact area compared with sample A. The differential conductance of sample B also shows a shift of the maximum of conductance to lower voltages comparable to sample A. In order to explain this effect, we again assume the NbO_x layer to be present between the Nb electrode and 2DEG. The damping of the conductance maximum is much stronger for sample B, which can be taken into account by assuming a shorter inelastic mean-free-path length in the electrode (see Sec. VI). A possible origin of the different behavior of the samples A and B may be the extreme roughness of the Nb electrode of sample B caused by the surface roughness of the InP after Ar sputtering, which was observed by scanning electron microscopy (SEM).

As is shown in Sec. VI, the high conductance of sample B at low voltages does not mean a much stronger amount of Andreev reflection compared with sample A. Instead, to explain this behavior, one has to assume the voltage drop to take place partially in the disturbed 2DEG of sample B near the contact to the Nb. This additional voltage drop enhances the subgap conductance of sample B, while the transmission probabilities of the interfaces in A and B are comparable. The disorder of the 2DEG is caused by the Ar cleaning with high ion energies. At the same time, the zero-bias anomaly (ZBA) inherent to disordered SN contacts[20] is not seen in the curve B, which can be explained by strong pair breaking in this disturbed part of the 2DEG. This effect in combination with the strong pair breaking in the Nb electrode shows that high-energy Ar cleaning is not suitable for observing high critical currents in S-Sm-S structures in our material system. Comparable experimental results have also been achieved for Ar-cleaned samples using a Pb/In alloy as the superconducting electrode.

Our further discussion is organized as follows. In Secs. IV and V details of the theoretical models of the proximity effect in A and B and their solutions are discussed. In Sec. VI the comparison of the experimental results with the theoretical models is given. Section VII presents the main conclusions of this study.

IV. MODELS

In this section, a detailed description of the models used later for the interpretation of the experimental data will be given. The properties of NS contacts with spatially homogeneous and equilibrium superconducting electrodes are presently well understood. The widely used model is based on the theory of Andreev and normal reflection processes at the NS interface developed by Blonder, Tinkham, and Klapwijk[17] (BTK model). In their approach, the current through a contact is fully determined by the amplitudes of normally and Andreev-reflected carriers at the NS interface. Later on, a microscopic derivation of the BTK model was presented independently by Zaitsev[21] and Arnold[22] by means of the Green's-function method.

The main source of deviations from the BTK model in real contacts are the effects of disorder. Namely, in the commonly used one-dimensional model the regime of conductance of the NS contact depends on the relation between the contact length along the current direction and the mean-free-path lengths in the contacting metals. The BTK model is applicable for a short (ballistic) contact when the potential drop takes place across the interface and the electrodes are in thermal equilibrium. In the opposite limit, when the contact length is larger than the mean-free-path lengths (disordered contact), the potential drop is distributed between the interface and the disordered region. This assumption leads to a nonequilibrium contribution to the conductance as discussed theoretically in Refs. 20,23–27. These two physically different situations are discussed below.

For the contact between the Nb and the clean 2DEG channel our physical model assumes that the two electrodes are weakly coupled by a (quasi-1D) interface. We further assume that, due to the smallness of the interface transmission coefficient, the potential drop takes place over the interface, and both electrodes are in thermal equilibrium. Next, we take into account explicitly the presence of a nonsuperconducting N layer on the Nb surface at the 2DEG-Nb interface. The structure therefore may be represented as an SN-2DEG junction, where N is a thin normally conducting layer at the surface of Nb and S is the bulk Nb electrode. Additionally, the proximity effect between the 2DEG and the SN electrode needs to be considered. Our approach is closely related to the original BTK one, in which the quasiparticle current through the contact is determined by the amplitudes of Andreev and normal reflections from the interface.[17] We note that in the considered case both kinds of reflection are determined by the local density of states (DOS) at the interface between the 2DEG and the N layer.[28,29] Thus the coefficients of Andreev and normal reflections are directly related to the energy spectrum of this disordered proximity N layer.

A physically quite different situation occurs when a disordered 2DEG channel exists between the clean 2DEG and the SN electrode. Then one may approximate this disordered region as a quasi-1D contact with a length along the current direction larger than the mean-free-path length. Properties of such disordered contacts have been first studied theoretically by Artemenko, Volkov, and Zaitsev[30] (short ScS constrictions) and more recently in Refs. 20, 23, 24, 26, and 27 ($NN'S$ contacts with a long disordered N' channel). In particular, an enhancement of the zero-bias conductance was predicted for these structures due to the interplay of Andreev and impurity scattering near the $N'S$ boundary. In the present paper we will apply these ideas to interpret the behavior of Ar-cleaned 2DEG-Nb contacts in which a disor-

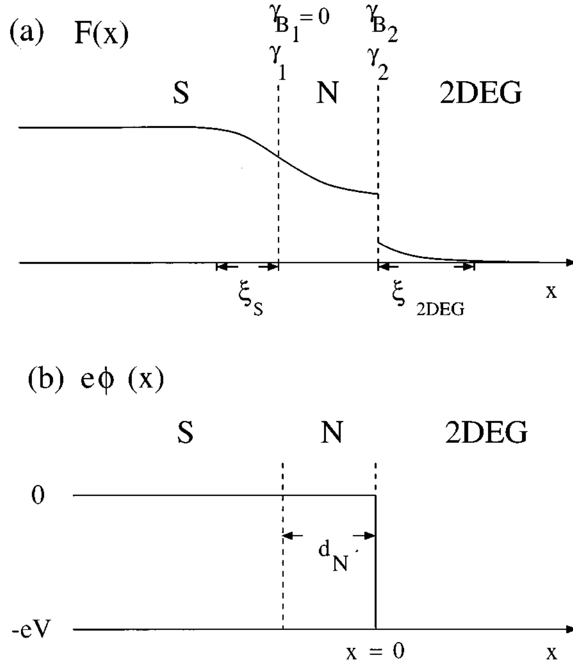

FIG. 3. Schematic presentation of the calculated layer sequence of the SN-2DEG model. The space dependence of the Cooper-pair density $F(x)$ (a) and of the potential drop (b) is shown. The parameters $\gamma_{1,2}$ are a measure for the suppression of $F(x)$ at the SN and N-2DEG interfaces, $\gamma_{B_{1,2}}$ describe the discontinuity in $F(x)$ at these interfaces.

dered region in the 2DEG channel near the interface with the Nb is produced.

We note that in both models of ballistic and diffusive contacts the one-dimensional representation is essentially used. In real distributed contacts inhomogeneities of the barrier strength may occur along the direction perpendicular to the current. Such inhomogeneities are excluded from our consideration.

The structure of the subsequent presentation is as follows. First we describe in more detail the models of ballistic and diffusive contacts and show how the current in both cases is related to the solution of the proximity effect problem. Second, the approach to the description of the proximity effect in a dirty SN bilayer will be formulated and some particular solutions will be given in order to illustrate the general trends. Next we will discuss the proximity effect in two more complicated layouts of ballistic and diffusive contacts separately.

A. Ballistic contact

The layout is shown schematically in Fig. 3. We consider the ballistic regime, i.e., such a situation when the size of the contact region between 2DEG and Nb (SN) electrode along the x direction is shorter than the mean free paths in the N and the 2DEG. This contact region is shown in Fig. 3 as an interface localized at $x=0$. We assume that the S and N metals are in the dirty limit $l_{S,N} \ll \xi_{S,N}$, whereas the 2DEG channel is in the clean limit.

We shall discuss the most general case, when both the 2DEG-N and the SN interfaces have nonzero normal reflection coefficients. The 2DEG-N interface is simulated by the BTK Z factor[17] related to the normal transmission coefficient D by $D=1/(1+Z^2)$.

For the clean ballistic 2DEG channel one may neglect the contribution of the channel to the total resistance. Then, because of the rather low transparency of the 2DEG/Nb interface due to a potential barrier caused by adsorbed hydrogen, fluoride, or a possible Nb_2O_5 oxide interlayer, the contact resistance is dominated by the 2DEG-N interface. In general, the Fermi velocity mismatch may also reduce the transparency. As a result, as shown schematically in Fig. 3, the whole potential drop eV takes place at the 2DEG/Nb interface, and the quasiparticle current across a contact is given by the following expression:[17]

$$I=\frac{e^2k_FW}{\pi^2\hbar}\int_{-\infty}^{\infty}[f_0(\epsilon+eV)-f_0(\epsilon)][1+A(\epsilon)-B(\epsilon)]d\epsilon, \quad (1)$$

where ϵ is the quasiparticle energy reckoned from the chemical potential, W is the contact width, k_F is the Fermi wavevector in 2DEG, and $A(\epsilon)$, $B(\epsilon)$ are the probabilities of Andreev and normal reflections at the 2DEG/Nb interface, respectively.

The microscopic derivation of the relations of $A(\epsilon)$ and $B(\epsilon)$ to the quasiparticle spectrum in the dirty SN electrode was made in Refs. 28 and 29. To analyze the processes of Andreev and normal reflection of a quasiparticle incident from a normal region into a disordered SN sandwich the solutions of the Gor'kov equations[31] in the N region have been matched with those of the Bogolubov–de Gennes (BdG) equations at distances smaller than l_N from the interface. It was shown that in the dirty limit the relation between the Bogolubov functions $u(\epsilon,x),v(\epsilon,x)$ and angle-averaged Green's functions $F(\epsilon,x),G(\epsilon,x)$ takes the simple form $v/u=iF/G$. One finally arrives at the following expressions for the Andreev reflection $A(\epsilon)$ and normal reflection $B(\epsilon)$ coefficients:[28,29]

$$A(\epsilon)=\frac{|F(\epsilon,x=0)|^2}{|1+2Z^2+G(\epsilon,x=0)|^2}, \quad (2)$$

$$B(\epsilon)=\frac{4Z^2(1+Z^2)}{|1+2Z^2+G(\epsilon,x=0)|^2}. \quad (3)$$

In the considered case $G(\epsilon,x=0)$ and $F(\epsilon,x=0)$ should be taken in the N region of the SN bilayer near the interface with the 2DEG.

The local density of states near the contact is given in the usual way as $N(\epsilon)=\mathrm{Re}\{G_\epsilon(\epsilon,0)\}$ which demonstrates explicitly the relation between $A(\epsilon),B(\epsilon)$ and the local quasiparticle spectrum in the N region. The function $|F(\epsilon,0)|$ may be interpreted as the density of states for Cooper pairs, as is suggested by Eq. (2). The expressions (2) and (3) generalize the corresponding BTK relations[17] for a spatially inhomogeneous case. In a spatially homogeneous case one has $G(\epsilon,0)=-i\epsilon/\sqrt{\Delta_0^2-\epsilon^2}$ and $F(\epsilon,0)=\Delta_0/\sqrt{\Delta_0^2-\epsilon^2}$, and Eqs. (2) and (3) are reduced to the BTK relations. Thus, according to Eqs. (1), (2) and (3) the current is determined by the Green's functions $G(\epsilon,0)$ and $F(\epsilon,0)$ and the problem

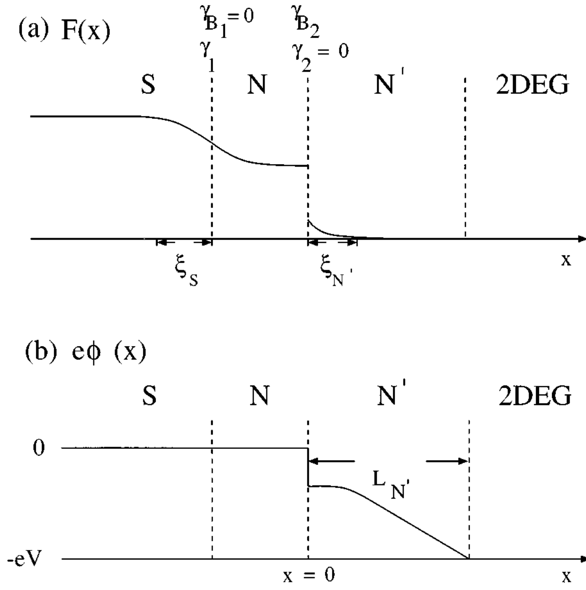

FIG. 4. Schematic presentation of the calculated layer sequence of the SN-N'2DEG model. The space dependence of the Cooper-pair density $F(x)$ (a) and of the potential drop (b) is shown. The parameters $\gamma_{1,2}$ are a measure for the suppression of $F(x)$ at the SN and N-N' interfaces, $\gamma_{B_{1,2}}$ describe the discontinuity in $F(x)$ at these interfaces.

is reduced to the solution for the proximity effect in the dirty SN sandwich including the influence of a clean 2D channel.

B. Diffusive contact

We model a diffusive 2DEG channel as a quasi-one-dimensional normal conductor N' of length $L_{N'}$ placed between a clean 2DEG and a superconducting SN reservoir (as previously, N denotes a possible proximity layer on the surface of Nb). We call the combination of the N'-N interface and the N' channel a diffusive contact between Nb and the clean 2DEG. The structure is therefore 2DEG-N'-NS (see Fig. 4). For the N'-N interface we consider the general case of finite transparency, whereas the contact between the disordered and the clean 2DEG channel (which in reality is rather a smooth transition) is assumed to have zero interface resistance.

The SN and 2DEG reservoirs are assumed to be in equilibrium having potentials 0 and eV, respectively. In contrast to the ballistic contact, the potential drop is not localized within the N'-N interface but is rather distributed between the N' conductor and the N'-N interface [see Fig. 4(b)]. The general approach to calculate the resistance of such structures was developed in Ref. 20. In the present paper this method will be applied to the study of I-V curves of the contact with the following extensions: (a) proximity effect and inelastic scattering in the N' channel and in the SN bilayer are taken into account; (b) the calculations are valid for arbitrary length of the N' channel, transparencies of the N'-N and the SN interfaces and temperatures, without additional approximations. Depending on the parameter range, the existence of different regimes will be demonstrated.

The quasiparticle current density across a contact is now given by the following expression:[20]

$$J=\frac{1}{eR_0}\int_{-\infty}^{\infty}[f_0(\epsilon+eV/2)-f_0(\epsilon-eV/2)]D(\epsilon)d\epsilon, \quad (4)$$

Here $R_0=R_{B_2}+R_{N'}$, where R_{B_2} and $R_{N'}=\rho_{N'}L_{N'}$ are the resistances per unit area of the N'-N interface and of the diffusive N' channel of length $L_{N'}$, respectively. $[2N_1(0)Ae^2v_{F1}]^{-1}$ is the contact resistance $D(\epsilon)$ is the effective transmission coefficient through the diffusive contact which contains contributions of subgap transmission due to Andreev reflection processes as well as of quasiparticle tunneling transport and is expressed in terms of the Green's functions G and F in the contact.[20] For our purpose it is convenient to introduce the function $\theta(\epsilon,x)=\theta_1(\epsilon,x)+i\theta_2(\epsilon,x)$ which is related to the Green's functions by $G(\epsilon,x)=\cos\theta(\epsilon,x)$, $F(\epsilon,x)=\sin\theta(\epsilon,x)$. Then $D(\epsilon)$ is given by the following expression:

$$D(\epsilon)=\frac{1+r}{\dfrac{r}{M(\epsilon)}+\dfrac{1}{L_{N'}}\displaystyle\int_0^{L_{N'}}\frac{dx}{\cosh^2\theta_2(\epsilon,x)}}, \quad (5)$$

where $r=R_{B_2}/R_{N'}$. The density of states factor

$$M(\epsilon)=\cos[\theta_1(\epsilon,x=0_+)-\theta_1(\epsilon,x=0_-)] \times\cosh\theta_2(\epsilon,x=0_+)\cosh\theta_2(\epsilon,x=0_-) \quad (6)$$

determines the contribution of the N'-N interface [0_+ and 0_- refer, correspondingly, to the N' and N regions in the vicinity of the interface at $x=0$, see Fig. 4(b)]. For $r\gg 1$ the transmission coefficient $D(\epsilon)$ is given by the product of the densities of states of N and N'. This demonstrates the crossover to the standard tunnel theory result. It is convenient to express r through the interface resistance parameter $\gamma_B=R_{B_2}/\rho_{N'}\xi_{N'}$ which yields $r=\gamma_B\xi_{N'}/L_{N'}$.

To summarize this section, the conductance of the diffusive contact 2DEG-N'-NS is expressed through the solutions for the proximity effect problem in the N' and SN regions. In the following these solutions will be described.

C. General description of the proximity effect in the dirty limit

As shown above, both diffusive and ballistic contacts, the current is determined by the solutions for the proximity effect problem. In this section the formalism for the proximity effect in the dirty SN sandwich is described and the physical parameters are introduced. Subsequently, the formalism will be applied to the particular cases of the ballistic and the diffusive Nb-2DEG contacts.

The Green's functions in the dirty limit obey diffusionlike equations[32,33] with the boundary conditions at the interface between superconducting and normal metals derived in Ref. 34. In terms of the function $\theta(\epsilon,x)$ introduced above, the equations for the Green's functions take a simple form:

$$\theta''(\epsilon,x)+\Delta(x)\cos\theta(\epsilon,x)+i[\epsilon+i\Gamma\cos\theta(\epsilon,x)]\sin\theta(\epsilon,x)=0, \quad (7)$$

where $\Delta(x)$ is the local value of the order parameter, and Γ is the pair-breaking rate due to inelastic or spin-flip scattering.

The boundary conditions at the SN interface have the form[34]

$$\gamma_B \xi_N \theta_N' = \sin(\theta_S - \theta_N), \tag{8}$$

$$\gamma \xi_N \theta_N' = \xi_s \theta_S'.$$

In the bulk of S θ_S is given by

$$\theta_S = \arctan(i\Delta_0/\epsilon), \tag{9}$$

where Δ_0 is the bulk value of the order parameter.

The self-consistency equation for the order parameter in the S region has the form

$$\Delta_s(x)\ln\frac{T}{T_c} + 2\frac{T}{T_c}\sum_{\omega_n}\left[\frac{\Delta_s(x)}{\omega_n} - \sin\theta_s(x,\epsilon=i\omega_n)\right] = 0, \tag{10}$$

where $\omega_n = \pi T(2n+1)$ are the Matsubara frequencies, and T is the temperature.

The parameters γ_B and γ

$$\gamma_B = \frac{R_B}{\rho_N \xi_N} = \frac{2}{3}\frac{l_N}{\xi_N}\left\langle\frac{1-D}{D}\right\rangle, \quad \gamma = \frac{\rho_S \xi_S}{\rho_N \xi_N} \tag{11}$$

have simple physical meanings: γ is a measure of the suppression of the order parameter in S due to the proximity effect between the S and N metals. This suppression is accompanied by the diffusion of Cooper pairs into N which is the origin of critical currents, e.g., in SNS or S-2DEG-S structures. γ_B describes the discontinuity in the Cooper-pair density, if the boundary transparency between these layers is smaller than unity. Here D is the normal transmission coefficient of the SN interface, the brackets $\langle\cdots\rangle$ denote angle averaging; $\rho_{S,N}$, $\xi_{S,N} = \sqrt{\mathcal{D}_{S,N}/2\pi T_c}$ and $\mathcal{D}_{S,N}$ are normal-state resistivities, coherence lengths, and diffusion constants of the S and N metals, respectively, while R_B is the interface resistance of the SN boundary.

Boundary conditions (8) can easily be adapted to any relevant specific cases. In particular, at the free interface (vacuum or insulator) $\theta' = 0$, whereas at the NS contact with $\rho_S/\rho_N \gg 1$ (large γ) one has $\theta = 0$.

The number of parameters may be reduced in the case of a thin N layer, $d_N/\xi_N \ll 1$. Then the parameters of the proximity effect problem are $\gamma_m \equiv \gamma d_N/\xi_N$ and $\gamma_B d_N/\xi_N$.

V. SOLUTIONS OF THE MODEL

A. Solutions for the ballistic 2DEG-NS contact

The ballistic contact consists of the disordered SN sandwich described above attached to the ballistic 2DEG channel. To simplify the problem the real 2D/3D contact is approximated by the quasi-one-dimensional structure shown in Fig. 3. This approximation does not change the results qualitatively, since it only leads to a redefinition of the parameters of the contact due to angle averaging, similar to the case of the 3D generalization of the BTK model.[35]

Due to the three-layer nature of the contact one needs to define two sets of boundary conditions: at the SN interface and at the 2DEG-N interface. For the SN interface the boundary conditions are given by Eq. (8) with γ_{B_1} and $\gamma_{m_1} = \gamma_1 d_N/\xi_N$. For the 2DEG-$N$ interface, which separates

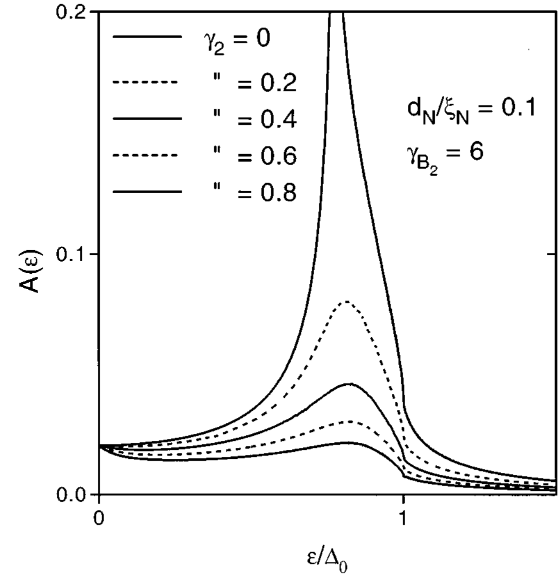

FIG. 5. The dependence of the Andreev-reflection coefficient $A(\epsilon)$ at the N-2DEG interface on the parameter γ_2, which describes the strength of the influence of the 2DEG to N.

the clean 2DEG and the disordered N regions, the definition (11) of the material-dependent parameters for boundary condition (8) does not hold. Instead, one may use the method of Ref. 36 to obtain the estimates for the proximity effect parameter $\gamma_2 \simeq (3p_{2\mathrm{DEG}}/p_N^2 l_N)\xi_N/\xi_{2\mathrm{DEG}}$. Here $p_{2\mathrm{DEG}}$ and p_N are the Fermi momenta in the 2DEG and in N, $\xi_{2\mathrm{DEG}}$ and ξ_N are the corresponding coherence lengths and l_N is the mean free path in N. Although in general $p_{2\mathrm{DEG}} \ll p_N$, this smallness may be partially compensated by the smallness of l_N. Therefore, one can put the upper limit for the parameter $\gamma_2 \leqslant 0.2$. This quantity is a measure of the influence of the 2DEG on the superconductivity in N and effectively plays the role of a pair-breaking parameter for N. The second proximity effect parameter describing the effect of normal transparency on the 2DEG/Nb interface is $\gamma_{B_2} = Z^2$, where Z is the barrier strength as defined in the BTK model. Qualitatively this is suggested by a comparison of the BTK relation $(1+Z^2) = D^{-1}$ with Eq. (11) in which the factor $\frac{2}{3}(l_N/\xi_N)$ may be dropped out in the clean limit. Details of the analysis will be published elsewhere.

As a result one arrives at the three-layer problem with two sets of boundary conditions, Eq. (8) for the SN interface and an analogous set at the N-2DEG interface with the parameters γ_2, γ_{B2}. This system of equations has been solved numerically. Inelastic scattering in the SN electrode can be taken into account by Γ_{SN} in Eq. 7. Using the solutions $\theta_N(\epsilon,x)$, one can calculate the local densities of states $N(\epsilon,x) = \mathrm{Re}\{\cos\theta_N(\epsilon,x)\}$ and $F(\epsilon,x)$ at any point of the system and therefore obtain the coefficients of Andreev reflection $A(\epsilon)$ and normal reflection $B(\epsilon)$ which determine the current according to Eqs. (1), (2), and (3).

Figure 5 shows the typical energy dependence of the Andreev reflection coefficient $A(\epsilon)$. The ratio $d_N/\xi_N = 0.1$ was used in these calculations. As is seen, for $\gamma_2 = 0$ a sharp peak exists which corresponds to the induced energy gap in N. With increase of γ_2 this peak is smeared out. In general, a second peak may exist at $\epsilon = \Delta_0$ for very small γ_{m_1}, as

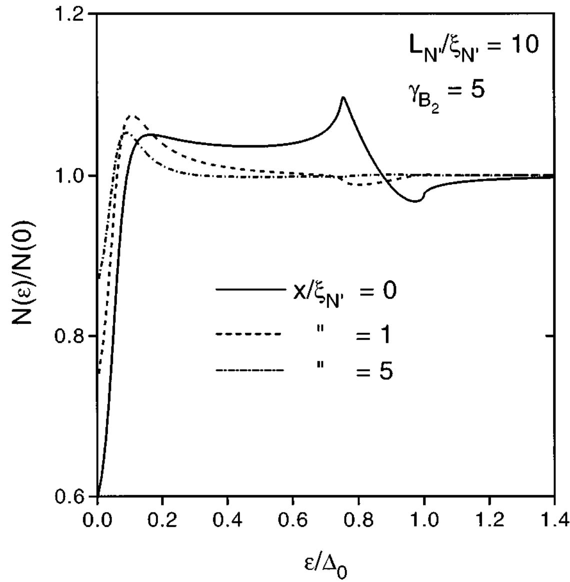

FIG. 6. Energy dependences of the normalized densities of states $N(\epsilon)$ in N' taken at local points at various distances $x/\xi_{N'}$ from the N-N' interface.

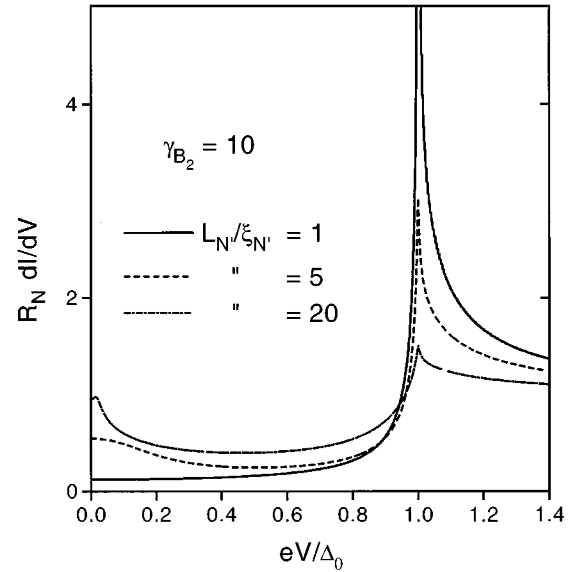

FIG. 7. The dependence of the zero-bias anomaly on the length $L_{N'}/\xi_{N'}$ of the disordered N' region.

discussed theoretically in Ref. 28 and observed, in the measurements of Nb-Si contacts in Ref. 10. This peak is not resolved in the considered case of rather large γ_{m_1} values.

B. Solutions for the diffusive 2DEG-N'-NS contact

The diffusive contact (see Fig. 4) consists of the disordered SN sandwich described above attached to the ballistic 2DEG channel via a disordered 2DEG channel (N') of length $L_{N'}$. Like in the previous case of the ballistic contact quasi-1D geometry is considered here.

Here the parameters γ_2 and γ_{B_2} refer to the combination of the disordered 2DEG channel (N') and N. In contrast to the previous case of the ballistic contact to the clean 2DEG, one may set $\gamma_2 = 0$ in the boundary condition at the 2DEG-Nb interface. The reason is that for the disordered N' channel the smallness of $p_{N'}/p_N \ll 1$ is not compensated by the large ratio of mean free paths as in the case of the clean 2DEG channel and N. Moreover, we will consider the most realistic case of vanishing barrier strength at the SN interface ($\gamma_{B_1} \ll 1$). We therefore have the following parameters of the model: the parameter γ_1 for the SN interface, γ_{B_2} for the N'-N interface, channel length $L_{N'}$ and pair-breaking parameters Γ_{SN} and $\Gamma_{N'}$ in Eq. (7). As mentioned above, the ratio of resistances that controls the regime of conductance, $r = R_{B_2}/R_{N'}$, is related to γ_{B_2} as $r = \gamma_{B_2}\xi_{N'}/L_{N'}$.

For arbitrary values of the parameters γ_1, γ_{B_2} the boundary value problem (7)–(9) was solved numerically. Some typical results of the calculations of the local densities of states $N(\epsilon,x)$ at low temperatures $T = 0$ in the N' region at different distances x from the N'-N interface are shown in Fig. 6. These densities of states demonstrate the gapless behavior in all regions of N'; however, they show a soft pseudogap for x of the order of several $\xi_{N'}$. With increasing x the position of a peak in the density of states shifts to lower voltages and saturates at the Thouless energy $\epsilon_T \sim \hbar \mathcal{D}_{N'}/L_{N'}^2$. The magnitude of the peak vanishes as $x \gg \xi_{N'}$, thus demonstrating the crossover to the normal behavior.

It is illuminating to demonstrate the appearance of the so-called zero-bias anomaly on the dI/dU curves. As is shown in Fig. 7, this enhanced conductance at small bias appears quite generally for a long channel $L_{N'} \gg \xi_{N'}$ provided that the transparency is sufficiently small ($\gamma_{B_2} \gg 1$). The physical origin of this enhanced conductance is an increase of the effective transmission coefficient $D(\epsilon)$ for the quasiparticles with small energy due to the contribution of superconducting correlations induced in the N' channel by the proximity effect. The manifestation of these correlations in the density of states is shown above in Fig. 6. This is consistent with theoretical results of Refs. 20, 23, 24, 26, 37, and 38 as well as with the experiment.[13] As is also seen from Fig. 8, the ZBA is destroyed quite rapidly with an increase of the pair-breaking rate, in accordance with earlier theoretical predictions of Refs. 20, 24 and 38. The pair-breaking rate of $\Gamma_{N'} = 0.2$ appears to be large enough to smear out the ZBA completely. This value is of the same order as determined experimentally from the comparison between the measurements and the model. Therefore we may conclude that the pair-breaking in the disordered part of the 2DEG is the reason why the ZBA was not observed in the present measurements.

VI. RESULTS AND DISCUSSION

We now compare the experimental results presented in Sec. III with our extensions to the BTK model (sample A) and to the model by Volkov *et al.*[20] (sample B) discussed in Sec. IV.

Figure 9 shows the normalized ($R_N \sim 1$ kΩ) differential conductance at 1 K of sample A (solid line) which was cleaned using 1 HF : 20 H_2O. The bias voltage is normalized here to the gap energy of the superconducting electrode,

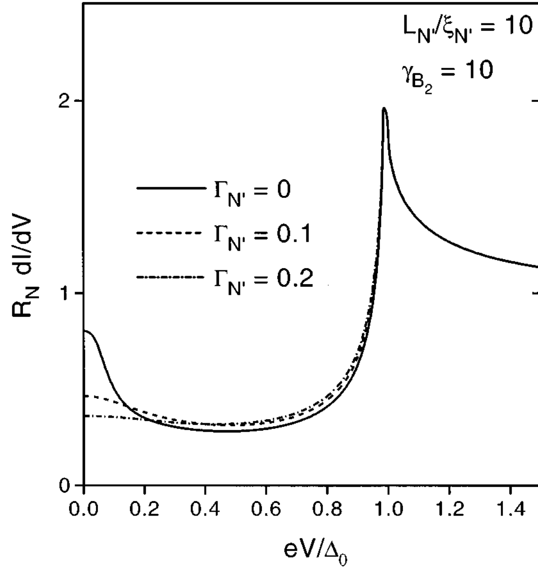

FIG. 8. The suppression of the zero-bias anomaly by inelastic scattering in the disordered N' region.

which was determined to be 1.38 meV by measuring its critical temperature. A fit using the BTK model (dashed line) shows a strong deviation from the measured curve. The only fitting parameter in the BTK model is the strength Z of the δ barrier at the interface between the superconductor and the semiconductor. The normalized zero-bias value is related to Z as $\sigma_{SN}(0)/\sigma_{NN}=2(1+Z^2)/(1+2Z^2)^2$. Inserting the measured zero-bias value we calculate $Z_{\mathrm{BTK}}=2$. The height and the position of the peak corresponding to the singularity in the density of states is obviously not well described by the BTK model.

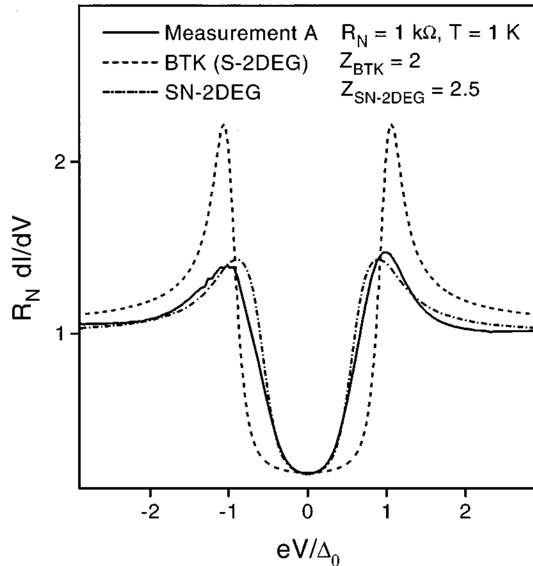

FIG. 9. Normalized differential conductance of a wet chemically cleaned sample with $R_N=1$ kΩ for $T=1$ K plotted versus the voltage drop at the interface in units of the Nb bulk gap (solid line). The BTK curve for $Z_{\mathrm{BTK}}=2$ is plotted for comparison (dashed line). Our fit is done for $\gamma_1=1.6$, $\gamma_2=0.2$, $\gamma_{B_2}=Z^2=6$, $d_N = 0.06\ \xi_N$ and $\Gamma_{SN}=0.07$ (dash-dotted line).

To explain this discrepancy we suggest some extensions to the BTK model towards a more realistic experimental situation. We include a dirty metal layer (N) between the Nb and the semiconductor surface in order to model a NbO_x ($x\sim 1$) layer. This metallic oxide is known to be formed as the first oxidation step of Nb surfaces up to a thickness of about 1 nm.[39] In addition, we assume a proximity effect between the superconducting electrode and the 2DEG channel which is always present if the electric contact is not highly resistive. As in the BTK model, we consider one-dimensional transport, equilibrium Fermi functions in S, N, and the 2DEG and a δ barrier at the N-2DEG interface.

We suppose that the NbO_x layer is formed by the first sputtered Nb atoms and a thin oxide layer that is built upon the semiconductor surface directly after the wet chemical cleaning, which was done outside the vacuum chamber. It was not possible to heat the sample in this chamber before depositing the Nb layer. This causes hydrogen and fluor still to be present on the surface what was proved by XPS spectra of similarly cleaned test samples. Additionally, it can be assumed that even in the sputter chamber some monolayers of H_2O and oxygen were adsorbed on the surface before the Nb deposition has started ($p\sim 1\times 10^{-6}$ mbar). This also supports the idea of formation of NbO_x. Between the NbO_x and the semiconductor surface the dielectric Nb_2O_5 can be formed if a sufficient amount of oxygen is present.[39] Nb_2O_5 can act here as a potential barrier between the superconducting electrode and the 2DEG.

Taking the above given assumptions into account, we have to calculate the differential conductance of an SN-2DEG structure, where N represents the conducting NbO_x layer. The proximity effect problem of the SN electrodes in an SN-c-NS structure was studied theoretically in Ref. 29. Here c denotes a geometrical constriction that causes the voltage drop measured in the experiment. In our case the whole voltage drop is assumed to take place at the N-2DEG interface [Fig. 4(b)] due to the insulating Nb_2O_5, adsorbates (fluor and hydrogen) from the wet chemical cleaning of the surface and due to the 3D-2D transition in this region (Sharvin resistance[40]). The difference in Fermi velocities of the metal and the semiconductor can be neglected as the origin of reflection at the interface because both are in the range of $v_F\sim 6-7\times 10^5$ m/s.

The calculation of the current given in Sec. IV is made by the method similar to that of BTK [see Eq. (1)]. The Andreev and normal reflection coefficients were determined at the interface between the N layer and the 2DEG using the local quasiparticle DOS at this position. This DOS mainly determines the shape of the differential conductance versus voltage dependence.

Figure 3(a) shows a schematic representation of the calculated layer sequence including the local values of the function $F(x)$ that can be identified with the Cooper-pair density. The variation of the Cooper-pair density at the boundary between the dirty metals ($l_{S,N}\ll\xi_{S,N}$, $l_{S,N}$ and $\xi_{S,N}$ are the elastic mean free path lengths and the coherence lengths in S and N) S and N (boundary 1) can be described by the parameters γ and γ_B given by Eqs. (11). These equations have to be modified for the boundary between N and the 2DEG (boundary 2) because the two-dimensional electron gas is assumed to be in the clean limit ($l_{\mathrm{2DEG}}\gg\xi_{\mathrm{2DEG}}$). A

more detailed discussion of this case is given in Sec. V A.

The strength of the suppression of the order parameter in S caused by the influence of N is characterized by the parameter γ_1. We expect that in our structure γ_1 should be of the order of unity because of the comparable carrier concentrations and elastic mean-free-path lengths in the polycrystalline Nb and the metallic Nb oxide. The results of the comparison between the model and experiment are shown in Fig. 9. The best fit was obtained with $\gamma_1 = 1.6$. Metals S and N should be in a good electrical contact, so we assumed a perfect transparency ($\gamma_{B_1} = 0$). The suppression of the Cooper-pair density causes a reduction of the gap in the quasiparticle DOS. This causes the shift of the conductance maximum in the measurement which is well described by our fit (Fig. 9, dash-dotted line). The thickness of the oxide layer can be estimated from the fit to be in the order of 1 nm. At the interface between N and clean 2DEG the proximity effect will be weaker due to the small effective mass in the 2DEG. For this reason the value of the parameter $\gamma_2 = 0.2$ as used in our fit can be estimated to be the upper limit (see Sec. V A). The transparency of this interface is given by the fitting parameter γ_{B_2} that cannot be estimated by the bulk material properties since it depends on the interface quality. From our fit we get a high value $\gamma_{B_2} = Z^2 = 6$ that corresponds to a low transparency $D_2 = (1+Z^2)^{-1} \sim 0.14$. This means the quality of the N-2DEG interface determines the normalized differential conductance for low voltages and especially at the zero bias, while the proximity effect between S and N causes the shift of the conductance maximum in the measurement.

The other feature of the measured curve that is not described by the BTK model is the height of the conductance maximum. Although the parameters Z and d_N also change the peak height, variation in the experimentally relevant range is not sufficient to fit the experimental data. The barrier strength Z additionally changes the zero bias and the thickness d_N of the N layer shifts the peak position. To account for the damping of the conductance peak we have to assume inelastic scattering in the SN electrode. The fit yields the scattering parameter $\Gamma_{SN} = 0.07$, which corresponds to the inelastic mean-free-path length of $l_{SN_{\mathrm{inel}}}$ of 1.4 μm. This result is of a realistic order of magnitude for T = 1 K if we extrapolate the inelastic mean-free-path length determined for Nb at 10 K in Ref. 41.

Another conclusion from the data analysis is, that a value of $Z = 2.5$ needed for the barrier strength to achieve a good fit, is larger than that estimated from the BTK model. That means that the amount of Andreev reflected holes is overestimated by simply deriving it from the zero-bias conductance. The difference is caused by the fact that in the BTK model each electron with energy below the gap energy is either normally or Andreev reflected. In our model the quasiparticle DOS is smeared out by the inelastic scattering and the proximity effect between S and N. As a result, low-energy subgap states are created and single electrons acquire a finite probability to enter the SN electrode for low voltages and even for zero bias. The probability for Andreev reflection is therefore reduced. In the limit of no Andreev reflection (normal DOS in N) the normalized zero-bias conductance is unity. That means for the same barrier strength the zero-bias conductance in our model is larger than in BTK.

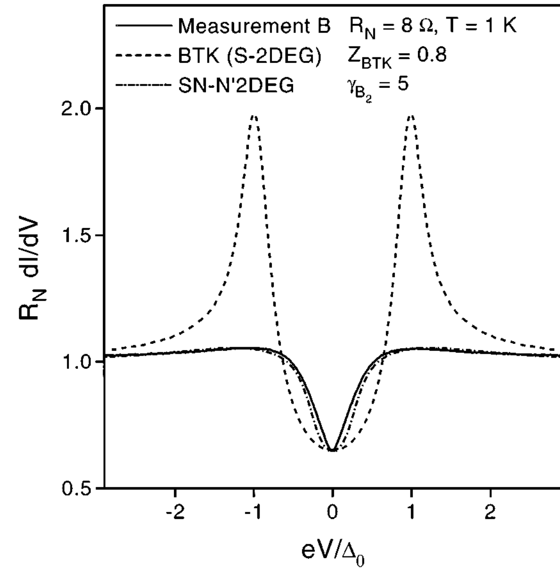

FIG. 10. Normalized differential conductance of a sample cleaned by 800-eV Ar ions with $R_N = 8\ \Omega$ for $T = 1$ K plotted versus the voltage drop at the interface in units of the Nb bulk gap (solid line). The BTK curve for $Z_{BTK} = 0.8$ is plotted for comparison (dashed line). Our fit is done for $\gamma_{m_1} = 0.15$, $\gamma_{B_2} = 5$, $L_{N'} = 7\ \xi_{N'}$, $\Gamma_{SN} = 0.26$ and $\Gamma_{N'} = 0.26$ (dash-dotted line).

As a consequence, the same zero-bias conductance in our model corresponds to a higher barrier at the N-2DEG interface than in the BTK model.

The experimentally measured contact resistance $R_N \sim 1$ kΩ is much higher than the value estimated for the contact width $W = 100\ \mu$m from the Sharvin formula, adding a barrier of the strength $Z = 2.5$. This can be explained by the effective length of the contact between the electrode and the 2DEG being much shorter than the geometrical one. It can be due to an inhomogeneity of the adsorbate barrier resulting from the wet chemical cleaning. As the current only flows through regions of lower barrier, the Z value has to be interpreted as an effective barrier strength of these contact regions.

Figure 10 shows the normalized ($R_N = 8\ \Omega$) differential conductance at 1 K of sample B (solid line) which was cleaned by Ar ions before depositing the Nb. For this sample, the deviation from the BTK model (dashed line, $Z_{\mathrm{BTK}} = 0.8$) is even more dramatic. We assume the high-energy Ar sputtering to be responsible. This cleaning process does not only remove the oxides that were formed on the semiconductor surface after the reactive ion etching process but also damages the 2DEG at the contact area. In the damaged region (now called N') the mobility of the 2DEG may be strongly reduced so that the measured voltage drop will take place not only at the interface between the SN electrode and N' but also in N' itself [see Fig. 4(b)]. Due to the background pressure of 10^{-6} mbar in the sputter chamber we assume NbO_x (N) and Nb_2O_5 layers to be present between the electrode S and the 2DEG similar to sample A. The voltage drop between SN and N' is now due to the 3D-2D Sharvin-resistance and due to the Nb_2O_5. To fit the measurement of sample B we have to model an SN-N'-2DEG structure that is schematically shown in Fig. 4(a). The gen-

eral approach that accounts for a nonequilibrium proximity effect on the N' conductor was developed by Volkov *et al.*[20] The relevant extension of this approach is presented in Sec. IV B.

The thickness of N determined from the fit of the sample A data yields $d_N/\xi_N \ll 1$. The effective parameter $\gamma_{m_1} = \gamma_1 d_N/\xi_N$ can now be used to describe the proximity effect between S and N. We can calculate $\gamma_{m_1} \sim 0.1$ using the values of $\gamma_1 = 1.6$ and $d_N = 0.06\ \xi_N$ determined above. This estimate is close to $\gamma_{m_1} = 0.15$, which gives the best fit, shown in Fig. 10 (dash-dotted line).

Besides the gap shift, the most striking feature is extremely strong damping of the conductance maximum for the Ar-cleaned sample B. In the model this can be accounted by shorter inelastic scattering length ($l_{SN_{\rm inel}} \sim 400$ nm) of the SN electrode. This assumption is reasonable due to the extremely rough InP surface after Ar-ion cleaning. This roughness is transferred to the Nb electrode as observed by SEM.

The proximity effect between N and N' can be neglected for sample B ($\gamma_2 = 0$) because of the lower mean free path length in N' after the ion damaging (see discussion in Sec. V B). This means there is no influence from N' to N which is associated in Fig. 4(a) with the constant Cooper-pair density in N near the interface to N'. The amplitude of the Cooper-pair density in N' at this interface depends only on the barrier strength. For the same barrier strength this Cooper-pair density would be even larger than that at the N-2DEG interface in the ballistic contact [Fig. 3(a)]. Nevertheless, supercurrents in S-2DEG-S diffusive devices should not necesseraly be larger than those in ballistic ones due to the shorter mean free path in the diffusive N' channel and the corresponding reduction of the coherence length $\xi_{N'}$.

For the case of a contact between two conductors in the dirty limit, the parameter γ_B is correlated with the interface transparency given by Eq. (11) but is not solely determined by $\langle D \rangle$. Due to the presence of the fraction $l_{N'}/\xi_{N'} \ll 1$ in the definition of γ_B, the relation $\gamma_B = Z^2$ provides only an upper estimate for this transparency. Here we extract $\gamma_{B_2} = 5$ for the contact between N and N' from the fit, or $Z \sim 2.3$. This is comparable with the value of sample A between N and clean 2DEG. That means that the overestimation of the amount of Andreev reflection when using the pure BTK model is even stronger for sample B than for sample A.

The conductance for low voltages for sample B is partially due to the disturbed 2DEG channel N'. The fit gives the length $L_{N'} = 7\ \xi_{N'}$ over which the potential profile is nearly linear. In this region the N' layer acts as a serial resistor with $R_{N'} = \text{const}$. Due to the influence of the superconducting electrode the electrical field is partially expelled at the distance of the coherence length $\xi_{N'}$ from the interface between N and N' [see Fig. 4(b)]. This may cause conductance enhancement called zero-bias anomaly at voltages $eV \ll \Delta_0$. For our values of $L_{N'}$ and γ_{B_2} one would expect to observe this ZBA in the measurement. Since this is not the case in our measurement, we attribute the ZBA suppression to pair breaking by inelastic scattering in N' (see Sec. V B). In Ref. 9, the inelastic scattering length for electron-electron scattering in a similar heterostructure with comparable properties was determined to be about 1 μm. Due to a possible decrease of the carrier concentration in the damaged N' the scattering length can be smaller there, which explains the value of $l_{N'_{\rm inel}} \sim 400$ nm obtained from the experimental fit.

Because of the uncertainty in electrical properties of the N and N' layers one may expect only approximate values for transparencies, scattering lengths, and layer thicknesses derived from the fits of both measurements. Deviations between fits and experimental curves may also be caused by inhomogeneities of the contact transparency that are not included in the one-dimensional models discussed here.

VII. CONCLUSIONS

In summary, we have measured the differential resistance of contacts between the superconducting Nb and the 2DEG in a $In_{0.77}Ga_{0.23}As$/InP heterostructure. Depending on the interface cleaning process, we observed rather different behavior of the contacts. We showed that within a realistic parameter range given by characteristic material parameters our models allow to describe the experimental data.

In the case of wet chemically cleaned samples, the shift and the damping of the conductance peak at $eV = \Delta_0$ could be modeled by assuming a normal conducting NbO_x layer (N) between Nb and semiconductor and pair-breaking effects present in this SN electrode. As an additional correction, the proximity effect between SN electrode and 2DEG was taken into account. The important result is that the amount of Andreev-reflected holes is overestimated by taking solely the zero-bias resistance value for the BTK model fit. The assumptions of the pure BTK model are not fulfilled here. Our fit of the experimental curves ends up in a much lower number of Andreev-reflected holes.

In the case of Ar-ion-cleaned samples we have shown that the voltage drop takes place partially in the disturbed 2DEG area. Due to inelastic scattering in this part of the 2DEG the zero-bias anomaly is not observed in our samples. The pair-breaking in the SN electrode as derived from the fit is stronger than in the case of wet chemically cleaned samples. This could be explained by InP surface roughness that influences the quality of the Nb electrode.

The measurements of samples prepared by different interface cleaning processes show the importance of a detailed physical understanding of the current transport through a semiconductor/superconductor interface. For example, the critical current in S-Sm-S devices can be reduced by pair-breaking in the SN electrode and in the disturbed semiconductor channel, as well as by normal oxide layers at the interface.

---

*Permanent address: Institute of Solid State Physics, 142432 Chernogolovka, Russia.

[1] T. D. Clark, R. J. Prance, and A. D. C. Grassie, J. Appl. Phys. **51**, 2736 (1980).

[2] W. M. van Huffelen, T. M. Klapwijk, D. R. Heslinga, M. J. de Boer, and N. van der Post, Phys. Rev. B **47**, 5170 (1993).

[3] A. W. Kleinsasser, T. N. Jackson, G. D. Pettit, H. Schmid, J. M. Woodall, and D. P. Kern, Appl. Phys. Lett. **49**, 1741 (1986).

[4] H. Takayanagi and T. Kawakami, Phys. Rev. Lett. **54**, 2449 (1985).
[5] K.-M. H. Lenssen, M. Matters, C. J. P. M. Harmans, J. E. Mooij, M. R. Leys, W. van der Vleuten, and J. H. Wolter, Appl. Phys. Lett. **63**, 2079 (1993).
[6] A. M. Marsh, D. A. Williams, H. Ahmed, Physica B **203**, 307 (1994).
[7] H. Takayanagi, T. Akazagi, J. Nitta, and T. Enoki, Jpn. J. Appl. Phys. **34**, 1391 (1995).
[8] H. Kroemer, C. Nguyen, E. L. Hu, E. L. Yuh, M. Thomas, and K. C. Wong, Physica B **203**, 298 (1994).
[9] J. Appenzeller, Th. Schäpers, H. Hardtdegen, B. Lengeler, and H. Lüth, Phys. Rev. B **51**, 4336 (1995).
[10] D. R. Heslinga, S. E. Shafranjuk, H. van Kempen, and T. M. Klapwijk, Phys. Rev. B **49**, 10 484 (1994).
[11] P. H. C. Magnée, N. van der Post, P. H. M. Kooistra, B. J. van Wees, and T. M. Klapwijk, Phys. Rev. B **50**, 4594 (1994).
[12] A. Kastalsky, L. H. Greene, J. B. Barner, and R. Bhat, Phys. Rev. Lett. **64**, 958 (1990).
[13] A. Kastalsky, A. W. Kleinsasser, L. H. Greene, R. Bhat, F. P. Milliken, and J. P. Harbison, Phys. Rev. Lett. **67**, 3026 (1991).
[14] A. W. Kleinsasser and A. Kastalsky, Phys. Rev. B **47**, 8361 (1993).
[15] C. Nguyen, H. Kroemer, and E. L. Hu, Appl. Phys. Lett. **65**, 103 (1994).
[16] B. J. van Wees, A. Dimoulas, J. P. Heida, T. M. Klapwijk, W.v.d. Graaf, and G. Borghs, Physica B **203**, 285 (1994).
[17] G. E. Blonder, M. Tinkham, and T. M. Klapwijk, Phys. Rev. B **25**, 4515 (1982).
[18] H. Hardtdegen, R. Meyer, M. Hollfelder, Th. Schäpers, J. Appenzeller, H. Løken-Larsen, Th. Klocke, Ch. Dieker, B. Lengeler, and H. Lüth, J. Appl. Phys. **73**, 4489 (1993).
[19] D. Uhlisch, A. A. Golubov, M. Hollfelder, K. Neurohr, A. V. Ustinov, A. I. Braginski, and H. Lüth, Czech. J. Phys. **46**, Suppl. S2, 657 (1996).
[20] A. F. Volkov, A. V. Zaitsev, and T. M. Klapwijk, Physica C **210**, 21 (1993).
[21] A. V. Zaitsev, Zh. Éksp. Teor. Fiz. **86**, 1742 (1984) [Sov. Phys. JETP **59**, 1015 (1984)].
[22] G. B. Arnold, J. Low-Temp. Phys. **59**, 143 (1985).
[23] A. V. Zaitsev, Pis'ma Zh. Éksp. Teor. Fiz. **51**, 35 (1990) [JETP Lett. **51**, 40 (1990)].
[24] A. F. Volkov, Pis'ma Zh. Éksp. Teor. Fiz. **55**, 713 (1992) [JETP Lett. **54**, 747 (1992)].
[25] B. J. van Wees, P. de Vries, P. Magnée, and T. M. Klapwijk, Phys. Rev. Lett. **69**, 510 (1992).
[26] C. W. J. Beenakker, Phys. Rev. B **46**, 12 841 (1992).
[27] A. F. Volkov, Phys. Lett. A **187**, 409 (1994).
[28] A. A. Golubov and M. Yu. Kupriyanov, Pis'ma Zh. Éksp. Teor. Fiz. **61**, 830 (1995) [JETP Lett. **61**, 851 (1995)].
[29] B. A. Aminov, A. A. Golubov, and M. Yu. Kupriyanov, Phys. Rev. B **53**, 365 (1996).
[30] S. N. Artemenko, A. F. Volkov, and A. V. Zaitsev, Solid State Commun. **30**, 771 (1979).
[31] A. A. Abrikosov, L. P. Gor'kov, and I. E. Dzyaloshinskii, *Methods of Quantum Field Theory in Statistical Physics* (Prentice Hall, Englewood Cliffs, NJ, 1963).
[32] G. M. Eliashberg, Sov. Phys. JETP **34**, 668 (1971).
[33] A. I. Larkin and Yu. N. Ovchinnikov, Zh. Éksp. Teor. Fiz. **68**, 1915 (1975) [Sov. Phys. JETP **41**, 960 (1975)].
[34] M. Yu. Kupriyanov and V. F. Lukichev, Zh. Éksp. Teor. Fiz. **94**, 139 (1988) [Sov. Phys. JETP **67**, 1163 (1988)].
[35] R. Hoonswat and I. M. Tang, Phys. Lett. A **127**, 441 (1988).
[36] M. Yu. Kupriyanov and V. F. Lukichev, Trudy FIAN **14**, 160 (1988).
[37] F. Zhou, B. Spivak, and A. Zyuzin, Phys. Rev. B **52**, 4467 (1995).
[38] Sungkit Yip, Phys. Rev. B **52**, 15 504 (1995).
[39] J. Halbritter, Appl. Phys. A **43**, 1 (1987).
[40] Yu. V. Sharvin, Zh. Éksp. Teor. Fiz. **48**, 984 (1965) [Sov. Phys. JETP **21**, 655 (1965)].
[41] M. Gurvitch, M. A. Washington, H. A. Huggins, and J. M. Rowell, IEEE Trans. Magn. **19**, 791 (1983).